

## 12 Particle Impact Phenomena

*Norman H. Tolk, Michael Albert, Justin Gregory, Glennys Mensing,  
Andrew Steigerwald, and Travis Wade*

- 12.1 Introduction 377**
- 12.2 Scattering from a Coulomb Potential 379**
- 12.3 Electron Impact 380**
  - 12.3.1 Interaction Mechanisms 380
    - 12.3.1.1 Collisions with Electrons in the Solid 380
    - 12.3.1.2 Scattering from the Lattice 382
    - 12.3.1.3 Bremsstrahlung 382
  - 12.3.2 Phenomena 383
    - 12.3.2.1 Plasmons 383
    - 12.3.2.2 Radiative Transitions 383
    - 12.3.2.3 Auger Processes 384
    - 12.3.2.4 Desorption Induced by Electronic Transitions (DIET) 385
    - 12.3.2.5 Secondary Electron Emission 385
  - 12.3.3 Applications 385
    - 12.3.3.1 Scattered-Beam Electrons 385
    - 12.3.3.2 Electrons from the Target 386
    - 12.3.3.3 Fluorescence Measurements 386
- 12.4 Ion Impact 386**
  - 12.4.1 Interaction Mechanisms 386
    - 12.4.1.1 Elastic Collisions with Target Atoms 386
    - 12.4.1.2 Collisions with Electrons in the Solid 387
  - 12.4.2 Phenomena 388
    - 12.4.2.1 Depth Dependence of Backscattering 388
    - 12.4.2.2 Sputtering 389
    - 12.4.2.3 Channeling 389
    - 12.4.2.4 Damage and amorphization 390
    - 12.4.2.5 Electronic Excitations 390
  - 12.4.3 Applications 390
    - 12.4.3.1 Measuring Beam Particles 390
    - 12.4.3.2 Recoil Target Atoms 390

- 12.4.3.3 Fluorescence Measurements 391
- 12.5 Photon Impact 391**
- 12.5.1 Interaction Mechanisms 391
- 12.5.1.1 Electronic Absorption 391
- 12.5.1.2 Nuclear Scattering 391
- 12.5.1.3 Coupling to Vibrational and Rotational Modes 391
- 12.5.2 Phenomena 392
- 12.5.2.1 Photoelectric Effect 392
- 12.5.2.2 Compton Scattering 392
- 12.5.2.3 Raman Scattering 392
- 12.5.2.4 Two-Phonon Absorption 393
- 12.5.2.5 Resonant Bond Breaking 393
- 12.5.2.6 Laser Ablation 393
- 12.5.2.7 Exciton Creation 393
- 12.5.2.8 Pockels and Kerr Effects 393
- 12.5.2.9 Coherent Phonon Generation 393
- 12.5.2.10 Sum Frequency Generation 393
- 12.5.3 Applications 394
- 12.5.3.1 Scattered or Absorbed Incident Light 394
- 12.5.3.2 Electrons from the Target 394
- 12.5.3.3 Measuring Scattered Light 395
- 12.5.3.4 Mode Locking Lasers 395
- 12.6 Neutron Impact 395**
- 12.6.1 Interaction Mechanisms 395
- 12.6.1.1 Scattering from Target Nuclei 395
- 12.6.1.2 Elastic Scattering from a Lattice 395
- 12.6.1.3 Neutron Activation 396
- 12.6.2 Neutron-Bombardment Phenomena 396
- 12.6.2.1 Phonon Emission and Absorption 396
- 12.6.2.2 Decay-Product Energy Loss 397
- 12.6.3 Applications 397
- 12.6.3.1 Elastic Scattering 397
- 12.6.3.2 Inelastic Scattering 397
- 12.6.3.3 Reaction Products 397
- 12.6.3.4 Spallation 397
- 12.7 Conclusion 398**
- Glossary 398
- References 400
- Further Reading 401

## 12.1 Introduction

In the past century, there has been a revolution in our understanding of the microscopic nature of matter, and much of this new insight was gained by observing the impact of beams of particles and photons on surfaces. Rutherford made his historic discovery of the nucleus by studying the scattering of a beam of  $\alpha$  particles as they passed through thin foils. Davisson and Germer confirmed the existence of de Broglie matter waves by observing the diffraction of a beam of electrons by crystalline targets. In fact, many of the most important experiments of the twentieth century relied on impact phenomena.

While high-energy particle beams continue to be the vanguard of research into the fundamental nature of matter, the techniques that played major roles in the development of modern physics have now become indispensable tools for materials analysis in nuclear, atomic, medical, and condensed-matter physics, as well as physical chemistry and materials science (Kittel, 2004). Much of the new technology that defines the modern world resulted from progress in these fields, and, in turn, this progress depends upon a basic understanding of impact phenomena. In fact,

impact phenomena play a prominent role throughout this Encyclopedia. This discussion, however, focuses on the rich variety of phenomena associated with beam interactions with condensed matter.

Analysis techniques that employ impact phenomena have in turn relied heavily upon progress made in related fields (Feldman and Mayer, 1986). Useful particle beams can only be produced in vacuum, and surfaces are difficult to characterize in the presence of air at normal temperatures and pressures. Therefore, vacuum technology has been particularly important to the development of impact techniques. Also, the emerging laser technologies and synchrotron-radiation sources are revolutionizing the way materials are characterized. Of course, progress in particle accelerator designs in both the high- and low-energy regimes has been crucial. Finally, the development of a tremendous variety of detectors and measurement devices has greatly expanded the range and sensitivity of experiments.

The nature of the interaction between a particle or photon beam and a target is highly dependent on the wavelength of the incident species. For a particle beam, the de Broglie relation gives the wavelength

$$\lambda = \frac{h}{\sqrt{2mE}} \quad (1)$$

where  $h$  is Planck's constant,  $m$  is the mass of the particle, and  $E$  is the energy (Shankar, 1994). The wavelength of a photon is just

$$\lambda = \frac{hc}{E} \quad (2)$$

where  $c$  is the speed of light. If the wavelength is much larger than the interatomic distance, then the incident particle wave function interacts with several target atoms at the same time. Consequently, in the infrared, visible, and ultraviolet atomic resolution is not possible. For photons, near-field techniques can circumvent this restriction to some extent. If the wavelength is the same order of magnitude as the interatomic distance in the target material, as it is in the X-ray region of the electromagnetic spectrum, then interference effects occur, allowing diffraction experiments, which can reveal periodic atomic structure. If the wavelength is much smaller, collisions can be characterized as simple two-particle interactions, and true atomic resolution is possible. Table 12.1 shows, for several beam species, the energy required to obtain wavelengths of 1 Å, which is about the size of an atom, and 5 Å, which is typical of interatomic distances in crystals.

As the table indicates, with photons only X-rays have short enough wavelength for diffraction experiments. Electrons, on the other hand, have a very convenient mass so that diffraction and atomic resolution are possible with modest energies easily

achieved in the laboratory. In contrast, nucleons have such large mass that interference effects are difficult to produce. Nevertheless, neutrons at thermal energies can be collimated into beams and used for diffraction experiments. For example, the energy for a 1-Å neutron given in the table would correspond to a temperature of 650 °C. This illustrates that each species has inherent difficulties and advantages.

Another central issue is the degree to which the probe itself modifies the target. Almost all experiments damage the target on a microscopic level, and high-energy or high-flux beams can do macroscopic damage. With the recent developments in constructing and characterizing nanostructures, minimizing even microscopic damage from analysis techniques has become crucial. Unfortunately, a useful description of damage requires a very thorough description of the extremely complicated dynamics and is beyond the scope of this chapter.

Section 12.2 describes the basic Coulomb interaction, which is the basis for most simple models of particle impact and is therefore applicable to several of the subsequent sections. The remaining sections are organized by the identity of the impacting beam. Section 12.3 treats electron bombardment. Section 12.4 deals with ion–solid interactions. Section 12.5 discusses photon interactions, and Section 12.6 presents neutron interactions. Although the chapter is organized in this manner, many of the concepts

**Tab. 12.1** The energy (in electron volts) required to achieve wavelengths of 1 and 5 Å for various species.

| Wavelength (Å) | Photon | Electron | Nucleon | Helium  | Argon    |
|----------------|--------|----------|---------|---------|----------|
| 1              | 12 400 | 150      | 0.0819  | ~0.02   | ~0.002   |
| 5              | 2 480  | 6.02     | 0.00328 | ~0.0008 | ~0.00008 |

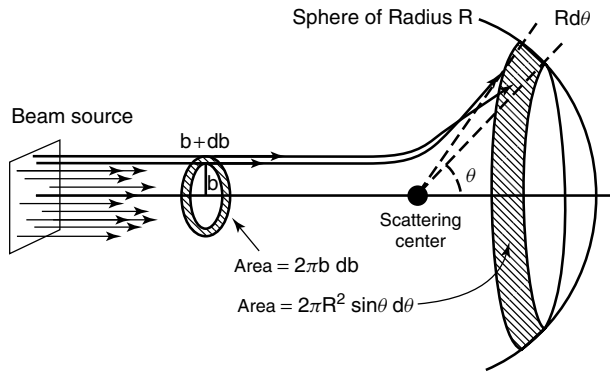


Fig. 12.1 The relationship between differential cross section and impact parameter.

of impact are applicable to more than one beam species. Within each section, the basic mechanisms of interaction are described, the observed phenomena are indicated, and finally, the most common applications are outlined.

## 12.2 Scattering from a Coulomb Potential

Many of the impact phenomena treated in this chapter begin with two-particle Coulomb scattering (Fetter and Walecka, 1980). Since this model is central to the discussion, a basic description is included. Charged particles traveling through a target material will feel a Coulomb repulsion or attraction to the electrons and nuclei in the material. Because materials are typically macroscopically neutral, it is assumed that long-range interactions are screened, and only individual classical two-particle collisions are significant. Because of the limited validity of this assumption, some of the later treatments will include correction factors that will not be derived.

Low-mass particles scattering from heavy target particles will transfer very little energy. Large scattering angles are possible, and scattering behavior can be

determined from the relation of impact parameter to scattering angle. The impact parameter  $b$  is defined as the perpendicular distance from the target particle to the initial line of flight. Figure 12.1 indicates the relationship between impact parameter and scattering angle. The differential cross section  $d\sigma$  can be defined by

$$d\sigma = 2\pi b db \quad (3)$$

From this model, it is seen that the differential cross section per unit solid angle is

$$\frac{d\sigma}{d\Omega} = \frac{b}{\sin \theta} \left| \frac{db}{d\theta} \right| \quad (4)$$

The integration of this over all solid angles yields the total cross section. The scattering problem is now reduced to determining  $db/d\theta$ , which can be inferred from the equations of motion in a Coulomb potential. In the center-of-mass frame, a particle with mass  $m$  and charge  $ze$  scattering from a particle of mass  $M$  and charge  $Ze$  will satisfy the equation

$$\mu \ddot{\mathbf{r}} = zZe^2 \frac{\mathbf{r}}{r^3} \quad (5)$$

where  $\mu$  is the reduced mass,  $\mu = mM/(M + m)$ , and  $\mathbf{r}$  is the vector from the

scattering center to the incident particle. The resulting orbits lead to the following relation between  $b$  and  $\theta$ :

$$b = \frac{|zZ|e^2}{\mu v^2} \cot \frac{\theta}{2} \quad (6)$$

where  $v$  is the velocity of the incident particle. Note that the sign of the charges is indistinguishable. With reference to Figure 12.1, an attractive potential would draw the particle down rather than push it up, but the scattering angle would be the same. Using this relation, the differential cross section may be written as

$$\frac{d\sigma}{d\Omega} = \left( \frac{zZe^2}{4E \sin^2(\theta/2)} \right)^2 \quad (7)$$

where  $E$  is the energy of the incident particle in the center-of-mass frame. If the scattering center is much more massive than the incident particle, the center-of-mass energy is approximately equal to the laboratory energy. Thus, this derivation is extremely useful for describing the scattering of light particles from heavy particles.

On the other hand, a heavy particle scattering from a light particle will change direction only slightly. In this case, the interesting parameter is the amount of energy transferred. Assume that the heavy particle does not deflect at all and that the interaction is sudden so that the target particle cannot move very much. The net impulse in the direction of travel is zero as a result of the symmetry of the incoming and outgoing paths. However, integrating the Coulomb force, the momentum transfer in the perpendicular direction  $\Delta p$  is

$$\Delta p = \frac{2zZe^2}{bv} \quad (8)$$

This then gives the transferred energy directly:

$$\Delta E = \frac{\Delta p^2}{2m} = \frac{mz^2Z^2e^4}{Mb^2E} \quad (9)$$

where the velocity of the incident particle has been written in terms of its kinetic energy:

$$E = \frac{1}{2}mv^2 \implies v^2 = \frac{2E}{m} \quad (10)$$

Equation (9) may be inverted to find the impact parameter in terms of the transferred energy. Using this for the impact parameter in Eq. (3), the differential cross section may be written in terms of the energy transfer as

$$d\sigma = \frac{\pi mz^2Z^2e^4}{ME\Delta E^2} d\Delta E \quad (11)$$

## 12.3 Electron Impact

### 12.3.1 Interaction Mechanisms

#### 12.3.1.1 Collisions with Electrons in the Solid

The interaction of a beam of electrons impinging on a solid or liquid target can be modeled to a good approximation by classical two-particle scattering from target electrons. Although the masses of the incident particle and target particle are identical, the impulse approximation applies if the energy of the incoming electron is sufficiently high. Here, the change in momentum  $\Delta p$  and thus the change in energy  $\Delta E$  as a function of impact parameter  $b$  reduce to

$$\Delta p = \frac{2e^2}{bv} \implies \Delta E = \frac{e^4}{Eb^2} \quad (12)$$

where  $e$  is the electron charge,  $v$  is the velocity of the incident electron, and  $E$  is the energy of the incident electron. Thus the differential cross section  $d\sigma$  is

$$d\sigma(E) = -2\pi b db = \left( \frac{\pi e^4}{E\Delta E^2} \right) d\Delta E \quad (13)$$

Integrating this gives the cross section for a particular transition with energy  $E_t$ :

$$\sigma = \pi \frac{e^4}{E} \left( \frac{1}{E_t} - \frac{1}{E} \right) \quad (14)$$

If the beam energy is much greater than the transition energy, the cross section simplifies to

$$\sigma \cong \frac{\pi e^4}{EE_t} \quad (15)$$

The possible electronic transitions are determined by the electronic structure of the target. The transition corresponding to  $E_t$  could be from a bound state, valence-band state, or conduction-band state to any higher energy state including free-particle states, which, if the surface is nearby, may result in the escape of electrons. For example, a valence-band electron could be promoted to the conduction band resulting in an electron-hole pair, or a bound core electron could be ejected from the solid.

Assuming that one transition dominates the absorption, the rate of energy loss as a function of distance traveled in the target may also be estimated by integrating energy times the differential cross section. This yields

$$-\frac{dE}{dx} = \frac{2\pi e^4 n}{E} \ln \left( \frac{E}{E_t} \right) \quad (16)$$

where  $n$  is the density of electrons in the initial state. Since energy can only

be transferred in discrete amounts, the mean free path can be estimated from the rate of energy loss. For example, the dominant interaction in a metal is plasmon excitation, and so the mean free path  $\lambda$  can be estimated from the plasmon energy  $\hbar\omega$ :

$$\frac{1}{\lambda} = -\frac{m\omega e^2}{2\hbar E} \ln \frac{4E}{\hbar\omega} \quad (17)$$

where  $m$  is the mass of the electron. For a 1-keV electron incident on a typical metal, this initial penetration depth is a few nanometers. This formula applies equally well to the escape depth of ejected electrons in the solid.

Note that the cross section and thus the mean free path depend on the energy of the incident particle. Since the particle loses energy after each collision,  $\lambda$  must be integrated to find the average range of travel of the incident electron in the target. This yields an equation for the path length (range)  $R$  of the form

$$R = \left( \frac{K}{\rho} \right) E^\gamma \quad (18)$$

where  $\rho$  is the density of the material and  $K$  and  $\gamma$  are constants. Since this derivation is approximate, the form of the electron range as shown in Eq. (18) is assumed, but the parameters  $K$  and  $\gamma$  are fitted empirically. The parameter  $K$  is dependent on the material's density and atomic weight, but for  $R$  in microns,  $\rho$  in grams per cubic centimeter, and  $E$  in electron volts the value for  $K$  is approximately 0.064 for all materials. The parameter  $\gamma$  depends on the target material and is typically between 1.2 and 1.7. While this estimates the length of the electron's trajectory, each interaction results in a random scattering angle so that the trajectory is generally not straight.

### 12.3.1.2 Scattering from the Lattice

Because of the wave nature of the incident electron, it may also scatter from the atoms in the target without exciting an electronic state. Quantum mechanically, the wave function interacts with many atoms at the same time (Wichmann, 1971). The scattered wave function interacts with itself, resulting in quantum interference effects, and scattering is enhanced in those directions for which the interference is constructive. Since the mass of the target is so much greater than the mass of the electron, the momentum transfer is negligible, and the electron will lose almost no energy. Electrons are well suited to diffraction studies of crystals because diffraction requires that the wavelength of the incident particle must be near the size of the structure to be investigated. At 150 eV, an electron will have a wavelength of about 11 Å. Electron backscatter diffraction (EBSD) has been used effectively for texture, stored energy, and grain characterization on small scales down to ~200 nm (Humphreys, 2004).

If the atoms in the target are regularly spaced in a lattice, the interference will also have a regular pattern. This can easily be demonstrated by considering Bragg reflection from adjacent planes of atoms (Figure 12.2). A beam reflecting from parallel planes separated by a distance  $d$  will

have a path-length difference of  $2d \sin \theta$ , where  $\theta$  is the angle of incidence. If these paths are such that constructive interference occurs, the path-length difference must equal an integer number of wavelengths:

$$n\lambda = 2d \sin \theta \text{ (Bragg condition)} \quad (19)$$

In a three-dimensional lattice, there are many ways to choose parallel planes of atoms, and each of these facets imposes another Bragg condition. Constructive interference will be greatest in scattering directions that best match all of these Bragg conditions, so that scattering in those directions is highly probable. On a detector screen, the set of favorable scattering directions forms a distinct pattern of points referred to as a *diffraction pattern*. The Bragg condition along with some simple geometry indicates that the distance between adjacent points in the diffraction pattern is inversely proportional to the distance between planes in the lattice.

### 12.3.1.3 Bremsstrahlung

In scattering from the target atoms, the incident electron is decelerated, and so it must emit radiation. While this is true for any charged particle, it is particularly important for electrons whose light mass readily allows them to experience large

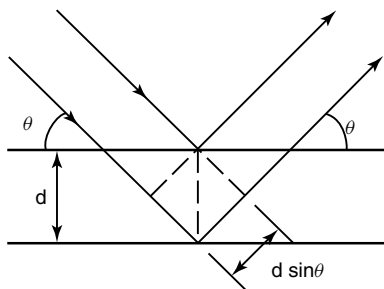


Fig. 12.2 Bragg reflection.

decelerations. A continuous spectrum of radiation will be produced in which the intensity decreases monotonically as a function of increasing energy up to the energy of the incident electron (Jackson, 1999). The radiation spectrum can be calculated from classical electromagnetic theory. For nuclear scattering of nonrelativistic electrons, the radiation spectrum is characterized by the Bethe–Heitler theory (Bethe and Heitler, 1934)

$$I = \frac{16Z^2 e^6}{3m^2 v^2 c^3} \times \ln \left( \frac{2 - (\hbar\omega/E) + 2\sqrt{1 - (\hbar\omega/E)}}{\hbar\omega/E} \right) \quad (20)$$

where  $I$  is the spectral intensity and  $Z$  is the atomic number of the target species. Note that the effect is greatest for high atomic number targets. The ratio of bremsstrahlung energy  $E_B$  to other losses is approximately

$$\frac{dE_B}{dE_{\text{other}}} \approx \frac{4Z}{3\pi 137} \left( \frac{v}{c} \right)^2 \quad (21)$$

For an energy of 100 keV and a target with  $Z \approx 30$ , roughly 4% of the beam power goes into bremsstrahlung.

### 12.3.2 Phenomena

#### 12.3.2.1 Plasmons

A plasmon is a density wave in the quasi-free gas of conduction electrons. It is important to note that electrons interact and produce correlated behavior in insulators as well as in metals; however, the following discussion applies only to metals. In metals, plasmon excitation will dominate the electron interactions. Consider a volume of negative charge embedded in a stationary positive charge of similar

volume. Displacing the negative charge creates a dipole field that in turn produces a linear restoring force. The plasmon is thus a harmonic oscillation with frequency

$$\omega = \sqrt{\frac{4\pi n e^2}{m}} \quad (22)$$

where  $n$  is the density of electrons. The energy of these oscillations is  $\hbar\omega$ . For typical metals, this falls in the range of 10–15 eV. Because of the surface boundary conditions, there is a separate surface-plasmon mode that has a characteristic frequency of  $\omega/\sqrt{2}$ . For very small particles, boundary conditions complicate the plasmon model, and the plasmon frequency will depend on the size and shape of the particle. Plasmons have been proposed for use as data interconnects in nanoscale transistors (Ozbay, 2006).

#### 12.3.2.2 Radiative Transitions

Electrons in the solid excited by impact may relax by emitting a photon. Also, if a core target electron is ejected, other electrons in the solid from either the same atom or neighbors may fall into the vacancy, emitting a photon. For radiative transitions, the energy of the photon will equal the difference in energy of the initial and final states of the radiating electron.

The easiest of these transitions to understand conceptually and interpret experimentally is a transition of a bound electron to fill a vacancy in the same atom. From perturbation theory, assuming only dipole interactions, the rate  $R$  for a spontaneous transition from a filled state to an empty state is found to be

$$R = \frac{4e^2}{3\hbar^4 c^3} \Delta E^3 | \langle f | \mathbf{r} | i \rangle |^2 \quad (23)$$

where  $\Delta E$  is the transition energy and the labels  $i$  and  $f$  refer to the initial and final electron states, respectively.

The rate depends heavily on the transition energy, but many transitions are disallowed by the dipole matrix element. Thus, the transition energy dependence is most apparent when comparing similar transitions in atoms with differing atomic number. The dipole matrix element between the initial and final state indicates that transitions between highly overlapping states are preferred. Since the change in angular momentum of the absorber (or emitter) must equal the angular momentum of the photon, the matrix element automatically imposes dipole selection rules. The allowed dipole transitions have  $\Delta l = \pm 1$  and  $\Delta j = \pm 1$  or 0, where  $l$  and  $j$  are the angular-momentum quantum numbers. However, other multipole transitions may occur with different restrictions.

12.3.2.3 Auger Processes

An electron making a transition to a core vacancy may also release the excess energy by exciting another electron. This is called an *Auger process*, and the resulting excited electron is called an *Auger electron* (Figure 12.3). The electron that falls into

the vacancy can most easily transfer energy to an electron in the same subshell. One falls into the vacancy, and the other carries the excess energy to a higher state, possibly the vacuum state, leaving two new vacancies in the higher shell or band. The transition rate also depends on the overlap of the initial and final states of the electron that fills the vacancy. Unlike radiative transitions, a vacancy may be filled by an electron from a higher orbital substate of the same primary shell as the vacancy. Since the initial and final states for such an intrashell transition are very similar, these transitions have higher rates than might be expected from the previous argument. These intrashell transitions are called *Coster-Kronig transitions*.

To first order, the energy of an escaping Auger electron can be estimated from the binding energies of the initial and final states. If a vacancy in state  $a$  is filled by an electron originally in state  $b$ , resulting in an electron in state  $c$  being ejected, the energy of the liberated electron is

$$E = E_a - E_b - E_c \tag{24}$$

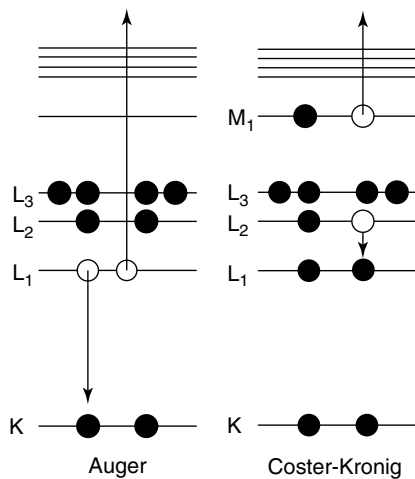


Fig. 12.3 Auger processes.

where these are the normal binding energies of the states. However, there is a significant correction due to the vacancies, which alter the normal binding energies. A fairly good estimate can be constructed from the binding energies of similar states in an atom with one more proton:

$$E = E_a^Z - E_b^Z - E_c^Z - \frac{1}{2} (E_c^{Z+1} - E_c^Z + E_b^{Z+1} - E_b^Z) \quad (25)$$

#### 12.3.2.4 Desorption Induced by Electronic Transitions (DIET)

When a *localized* excited state is created in a solid, it dramatically changes the local electronic environment. If the state is sufficiently long lived, the electromagnetic forces can alter the position of an atom or molecule in the lattice, resulting in defect formation or even desorption (Tolk *et al.*, 1983). Consider an atom adsorbed on a surface. An electron in some bonding orbital holds the atom to the surface. If that electron is excited to a weaker-bonding or even an antibonding state, the bond may break, resulting in desorption. Somewhat more spectacular is the highly repulsive state that results when the electron of one atom makes a transition into the core vacancy of a neighboring atom. Several other mechanisms exist by which the electronic energy can be channeled into the kinetic energy of the atoms or molecules in the lattice, resulting in damage.

#### 12.3.2.5 Secondary Electron Emission

In addition to directly ejected electrons or Auger electrons, a target will also emit a broad band of electrons with energies less than 100 eV that are relatively insensitive to the energy of the incident beam. These low-energy electrons are called *secondary electrons* because they clearly

do not result from a single-step process or even a two-step process like Auger electrons. Although secondary electrons arise from several sources, an argument based on plasmons provides a clue to their origin. One or more plasmons may couple to a single electron, thus giving that electron enough energy to escape from the surface. Since plasmons have fixed energies, the shape of the energy spectrum of emitted electrons would not depend on how the plasmons were created. This and other similar processes result in an energy spectrum of which only the amplitude depends on the incident energy.

#### 12.3.3 Applications

##### 12.3.3.1 Scattered-Beam Electrons

Since the probability for electron scattering depends on the density of electrons in the material, the scattering of electrons for a fixed target thickness will vary with different materials. For example, this effect provides the contrast for transmission electron microscopy (TEM).

The incident electron can only lose energy in discrete amounts determined by the allowed transitions in the target material. Thus, one can learn a great deal about the electronic structure of the target by measuring the energy of beam electrons that pass through the target. This is the basis of electron energy-loss spectroscopy (EELS). If the same measurement is made for the reflected portion of a low-energy beam, the measurement is surface sensitive. This is the principle behind high-resolution electron-energy-loss spectroscopy (HREELS).

Since elastically scattered electrons may interfere, the structure of the lattice can

be determined from the spatial distribution of scattered electrons. This is the basis of electron diffraction. For example, the transmitted-beam electrons in a transmission electron microscope demonstrate a diffraction pattern. Low-energy electrons reflected at normal incidence from a crystalline surface will also show a diffraction pattern, which is primarily surface sensitive. This is called *low-energy electron diffraction (LEED)*. Because the component of energy into the surface is small, a high-energy electron beam reflected at grazing incidence will also produce a surface-sensitive diffraction pattern. This technique, called *reflection high-energy electron diffraction (RHEED)*, provides a more convenient geometry than LEED in that the surface is more accessible for simultaneous experiments.

#### 12.3.3.2 Electrons from the Target

In addition to scattered-beam electrons, Auger electrons may also escape from the target. Measuring the energy of electrons reveals peaks at energies corresponding to the Auger transitions, which are characteristic of the target atoms. Thus Auger-electron spectroscopy (AES) can detect target species down to the 0.1% level. Elaborate techniques are usually required to separate the Auger peaks from the background of scattered-beam electrons.

#### 12.3.3.3 Fluorescence Measurements

To avoid the background problem of Auger-electron spectroscopy, the characteristic photons produced by similar radiative transitions may be detected. Since the size of the target volume probed by the electron beam can be reduced to about a micron, this technique is referred to as *electron microprobe analysis (EMA)*. Characteristic photons are typically in the hard ultraviolet

or X-ray region and thus have their own detection challenges.

## 12.4 Ion Impact

### 12.4.1

#### Interaction Mechanisms

##### 12.4.1.1 Elastic Collisions with Target Atoms

Particles such as ions or molecules striking a surface will interact primarily by elastic collisions with target atoms. By conservation of energy and momentum, it is easily shown that the fraction of initial energy retained by the incident particle is

$$\frac{E_1}{E_0} = \left[ \frac{(M_2^2 - M_1^2 \sin^2 \theta)^{1/2} + M_1 \cos \theta}{M_1 + M_2} \right]^2 \quad (26)$$

where  $M_1$  is the mass of the incident particle,  $M_2$  is the mass of the target particle, and  $\theta$  is the scattering angle. This ratio is referred to as the *kinematic factor* and is often denoted by  $K$ . The kinematic factor as a function of angle for several choices of the ratio  $M_2/M_1$  is plotted in Figure 12.4 The fraction of energy transferred to the target particle is similarly given by

$$\frac{E_2}{E_0} = \frac{4M_1M_2}{(M_1 + M_2)^2} \cos^2 \phi \quad (27)$$

where  $\phi$  is the recoil angle. For particular scattering angles, these relations become quite simple. For example, in the case of backscattering,  $\theta = \pi$  and  $\phi = 0$ , so

$$\frac{E_1}{E_0} = \left( \frac{M_2 - M_1}{M_1} \right)^2 \quad \text{and} \quad \frac{E_2}{E_0} = \frac{4M_1M_2}{(M_1 + M_2)^2} \quad (28)$$

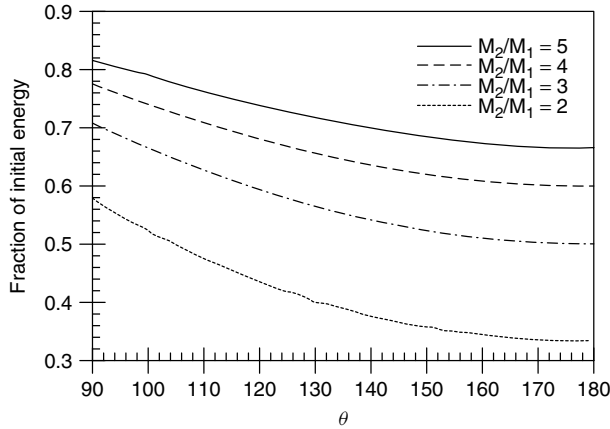


**Fig. 12.4** The kinematic factor as a function of scattering angle for several choices of the ratio  $M_2/M_1$ .

Electron screening of target nuclei complicates heavy particle scattering. Nevertheless, if the energy of the incident particle is high enough to penetrate well within the electron cloud, the simple scattering model will be approximately correct. This condition will be met if

$$E_0 > \frac{zZe^2}{a_0} \quad (29)$$

where  $z$  is the atomic number of the incident atom,  $Z$  is the atomic number of the target species, and  $a_0$  is the Bohr radius. In any case, screening will produce some deviation from the simple model, and, in general, a correction factor must be included. Ignoring electron screening, the cross section is as given above:

$$\sigma(\theta) = \left( \frac{zZe^2}{4E \sin^2(\theta/2)} \right)^2 \quad (30)$$

#### 12.4.1.2 Collisions with Electrons in the Solid

An incident heavy particle will also collide with electrons in the solid. However, as a result of momentum conservation, a heavy particle can transfer only a small fraction of its momentum to an electron. Thus, as

a high-energy particle traverses a target, it will slowly lose energy through numerous electron collisions in an almost continuous fashion. These collisions may also be modeled with the impulse approximation. The derivation of the rate of energy loss is completely analogous with that for electron-electron scattering. Thus the rate of energy loss as the particle traverses the target is

$$-\frac{dE}{dx} = \frac{2\pi z^2 e^4 n}{E} \frac{M}{m_e} \ln \frac{4Em_e}{IM} \quad (31)$$

where  $M$  is the mass of the incident particle,  $z$  is its atomic number,  $I$  is the average excitation energy of electrons in the solid, and  $n$  is the density of electrons in the solid.  $I$  is complicated, but, for heavier elements, it is approximately equal to  $10Z$ . This is usually converted to a “stopping power” per atom (Figure 12.5). The stopping power  $\varepsilon$  per atom is defined as

$$\varepsilon = \frac{dE/dx}{N} \quad (32)$$

where  $N$  is the density of the target atoms. The stopping power can then be used to determine  $dE/dx$  for compounds.

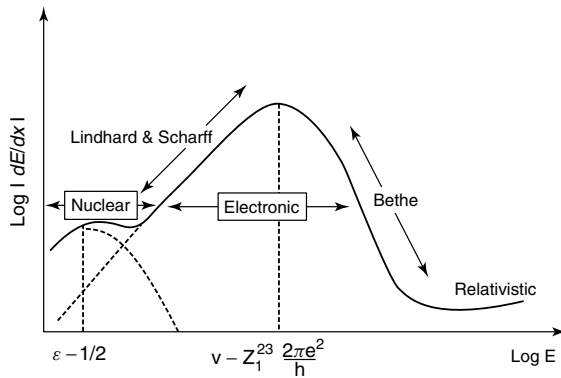


Fig. 12.5 Stopping power.

According to Bragg's rule, for a compound  $A_n B_m$ , the stopping power is

$$\varepsilon_{A_n B_m} = n\varepsilon_A + m\varepsilon_B \quad (33)$$

where  $n$  and  $m$  are the relative atomic abundances of the respective constituents. Thus, multiplying by the molecular density, the rate of energy loss in a compound target may be determined.

Although electronic stopping is the most important contribution to the energy loss for a large range of energies, other factors such as scattering from the atomic cores are also important. The convoluted path resulting from numerous scattering events further complicates this picture. To compute the total depth beneath the surface attained by an incident particle,

all of these factors must be considered. Table 12.2 indicates the median penetration depth for various species and energies of particles incident on amorphous alumina.

#### 12.4.2 Phenomena

##### 12.4.2.1 Depth Dependence of Backscattering

Since a heavy particle will lose energy to electrons as it penetrates a target, the electron scattering produces depth dependence in the energy of atomic scattering. For example, consider a light ion with energy  $E$  scattering from an atom at a depth  $d$  within the target. To find the total energy lost to electron scattering,  $dE/dx$

Tab. 12.2 Penetration depth in  $\mu\text{g}/\text{cm}^2$  for various incident species and energies, derived from implantation of amorphous alumina.<sup>a</sup>

| Energy (eV) | Na  | K   | Kr  | Xe  |
|-------------|-----|-----|-----|-----|
| 10          | 4.5 | 2.6 | 2.5 | 2.3 |
| 100         | 35  | 20  | 14  | 11  |
| 1000        | 500 | 260 | 170 | 100 |

<sup>a</sup> (Jespégard and Davies, 1967).

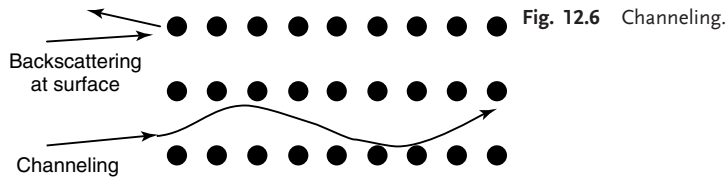


Fig. 12.6 Channeling.

should be integrated to the penetration depth. However, for modest depths, the fractional energy loss will be small, and the total energy loss is approximately

$$\Delta E \cong \frac{dE}{dx} d \quad (34)$$

where  $dE/dx$  is evaluated at the incident energy  $E$ . The particle with this reduced energy now backscatters from a target atom, and the energy is reduced by the kinematic factor above. The particle then traverses the target again before escaping. Since the particle may have been scattered at an angle to the surface normal, the distance traveled on the way out is  $d/\cos\theta$ . The energy loss is approximated as above with  $dE/dx$  now evaluated at the appropriate backscattered energy. Thus, the total energy lost to the electrons both in entering and exiting the sample is

$$\Delta E = d \left( K \frac{dE}{dx} \Big|_{\text{in}} + \frac{1}{|\cos\theta|} \frac{dE}{dx} \Big|_{\text{out}} \right) \quad (35)$$

where  $K$  is the kinematic factor and “in” and “out” indicate at which energy  $dE/dx$  should be evaluated. Note that the total energy lost to electron scattering is directly proportional to the penetration depth.

#### 12.4.2.2 Sputtering

Atomic collisions impart significant energy to the target atoms, and, in general, they will in turn collide with other target atoms. The resulting collision cascade can give some atoms sufficient momentum to escape from the target, and so the ion beam erodes the target. This process

is called *sputtering* (Behrisch, 1981). The sputtering yield is defined as the number of target atoms emitted per incident particle. This depends not only on the nature of the target material but also on the beam species and energy, and the possible values vary tremendously. Although calculation of sputtering yields is understandably daunting, theory has produced good results. Nevertheless, for practical applications, empirical values are used.

#### 12.4.2.3 Channeling

If the target is crystalline, an interesting phenomenon known as *channeling* may occur (Figure 12.6). If the incident particles are aligned along one of the highly oriented directions of the crystal, they cannot collide solidly with atoms in the bulk of the target. Essentially, the atoms on the surface shadow the rest of the atoms. However, the effect is greater than that simple explanation indicates. Consider the regular lattice to be parallel planes of atoms. If the incident particle is moving nearly tangential to these planes, it will merely glance off the planes at a shallow angle. This requires very little energy, and the incident particle will move down this channel, making a series of shallow collisions with the “walls”. Thus, a particle incident in a channeling direction may penetrate very deeply into the target. The ultimate depth achieved is primarily determined by electron stopping. Furthermore, backscattering will only occur at the surface.

#### 12.4.2.4 Damage and amorphization

For sufficiently energetic ion beams, energy loss can occur through defect creation. Depending on the temperature during ion bombardment, both point and complex defects may be created. Consequences include deteriorated electronic and optical properties, a problem especially relevant in high-energy particle detectors (such as at LHC or GANIL). For increased dosage, enough damage may occur such that the amorphous state becomes energetically favorable. However, this threshold varies with relative target-ion mass difference, temperature, and dosage. Finally, many materials exhibit interesting nonlinear behavior when irradiated with swift (0.1–1 GeV) ions. Such effects include latent tracks and phase changes to metastable lattice configurations.

#### 12.4.2.5 Electronic Excitations

In colliding with the electrons, a heavy particle excites electronic states in the target just as in the case of electron bombardment. Therefore, many of the same phenomena are seen in each case. Electrons will be ejected, electron–hole pairs will be created, plasmons will be stimulated, secondary electrons will be produced, and most of the other previously discussed electronic excitations will occur. Of particular interest are the radiative transitions to fill a core hole created by the incident particle. The origins of the core hole are irrelevant, and the process is exactly as described in the Section 12.3.

### 12.4.3

#### Applications

##### 12.4.3.1 Measuring Beam Particles

The energy of a light ion that has been scattered is uniquely determined by

the species from which it scattered. If the energy of scattered-beam particles is measured, the composition of the target can be determined. This is the basis of Rutherford backscattering spectrometry (RBS). For simplicity, the measurement is usually made as close to the backscattering direction as possible. Since the energy has a simple dependence on depth due to electron scattering, depth profiling is also possible. Finally, since subsurface atoms cannot readily backscatter when the beam is aligned along a channeling direction, channeling can enhance the surface sensitivity of RBS. For example, RBS can easily detect whether a surface is reconstructed, relaxed, or covered with an adsorbate.

To enhance surface sensitivity, an ion beam with energy in the range of one to a few kiloelectron volts may be used in conjunction with an electrostatic energy analyzer. Since particles that penetrate the surface are almost always neutralized, the electrostatic energy analyzer will detect only particles scattered from the surface. The low-energy beam ensures that most of the ions will be scattered from the surface. This is the basis of low-energy ion scattering (LEIS).

##### 12.4.3.2 Recoil Target Atoms

Backscattering is inefficient for lighter target materials and kinematically impossible if the target material is lighter than the beam species. Rather than measuring backscattered beam particles, measuring the energy of forward recoiling target atoms gives the same kinematic information. This is the basis of forward recoil spectrometry (FRS). The beam is usually incident at a shallow angle to the target surface, and the recoiling atoms are detected at some small angle from the surface in the forward direction.

### 12.4.3.3 Fluorescence Measurements

Heavy particles may also produce core-hole vacancies in target atoms. The mechanisms for filling the vacancy are exactly the same as described above. In particular, the target may be characterized by measuring the radiation from such transitions. This is the basis of proton- (or particle)-induced X-ray emission (PIXE). Because the larger mass of the incident particle results in far less bremsstrahlung, PIXE has less background noise than electron microprobe analysis.

## 12.5 Photon Impact

### 12.5.1

#### Interaction Mechanisms

##### 12.5.1.1 Electronic Absorption

A photon incident on a target atom or molecule may excite higher electronic states in the target. If the photon is modeled as an oscillating perturbation  $H' e^{-i\omega t}$ , from first-order perturbation theory, the probability of stimulating a transition is given by Fermi's "golden rule,"

$$P_{i \rightarrow f} = t \frac{2\pi}{\hbar} |\langle f | H' | i \rangle|^2 \delta(E_f - E_i - \hbar\omega) \quad (36)$$

where  $t$  is the length of time that the perturbation is applied, and the labels  $i$  and  $f$  indicate initial and final states of the *unperturbed* system. The terms  $E_i$  and  $E_f$  are the energies of the unperturbed initial and final states. Note that the transition energy must be equal to the energy of the photon. This seems to imply that the whole photon must be absorbed, and scattering will not occur. However, the excited state may relax by emitting another photon with either equal or lower energy, resulting in an

effective scattering. Also, according to the uncertainty principle, noneigenstates can exist for a short time, so photons may be scattered even when no resonant transition exists. Nevertheless, the probability of interaction is much greater at resonance, that is, when there exists a transition with a difference in energy equal to the energy of the photon. Therefore, light will be strongly absorbed at frequencies that correspond to the allowed electronic transitions. The matrix element indicates the strength of coupling of the photon to the electronic states. In general, the coupling is proportional to the dipole moment. However, as in the case of atomic hydrogen, time dependence allows some coupling where no dipole moment exists. Finally, because a photon has angular momentum, only transitions with  $\Delta l = 1$  are allowed with high probability in the dipole approximation.

##### 12.5.1.2 Nuclear Scattering

An incident photon may also scatter from the target atom without leaving the atom in an excited state. The large mass of the nuclei allows momentum to be conserved without significantly changing the energy of the photon. Since the energy does not change, the photon maintains its initial wavelength, and interference may occur. As with electrons, the resulting diffraction pattern is indicative of the long-range order of the target. The diffraction relations are exactly the same as discussed previously for particle interference (see Section 12.3.1.2).

##### 12.5.1.3 Coupling to Vibrational and Rotational Modes

Molecular bonds may have many modes of vibration and rotation, each with one or more natural frequencies. If a given

bond has electric dipole characteristics, the electric field of a photon with a frequency resonant to the bond may excite these bonds to higher vibrational and rotational states. A photon is absorbed in the process.

### 12.5.2 Phenomena

#### 12.5.2.1 Photoelectric Effect

If the incident photon has greater energy than the binding energy of electrons in the target, electrons may be liberated. The maximum energy of the ejected electron will be

$$E = E_b - \hbar\omega \quad (37)$$

where  $E_b$  is the binding energy of the electron. Since the final state is a free particle, selection rules can always be satisfied, and all electrons with binding energy less than or equal to the photon energy may be liberated. Applying Fermi's "golden rule" to hydrogenic states yields the cross section for a photon of energy  $\hbar\omega$  liberating an electron with binding energy  $E_b < \hbar\omega$ :

$$\sigma = \frac{128\pi e^2 \hbar E_b^{5/2}}{3mc(\hbar\omega)^{7/2}} = \frac{7.45 \text{eV}\text{\AA}^2}{\hbar\omega} \left(\frac{E_b}{\hbar\omega}\right)^{5/2} \quad (38)$$

#### 12.5.2.2 Compton Scattering

For photon-electron scattering, if the energy transferred to the electron is much greater than its binding energy, the scattering will be nearly identical to scattering from a free electron. The resulting scattering behavior can be deduced simply from energy and momentum conservation. If a photon initially with energy  $\hbar\omega$  scatters at an angle  $\theta$  from an electron initially at rest,

conservation of energy requires

$$E_p + E_e = E'_p + E'_e \implies \hbar\omega + mc^2 = \hbar\omega' + E' \quad (39)$$

where the subscripts refer to photon and electron, and unprimed and primed stand for before and after the collision, respectively. The term  $E'$  is the subsequent relativistic energy of the electron. Momentum conservation requires

$$\mathbf{p}_p = \mathbf{p}'_p + \mathbf{p}'_e \implies (\mathbf{p}_p - \mathbf{p}'_p) = \mathbf{p}'_e \quad (40)$$

which may be written as

$$\frac{\hbar^2\omega^2}{c^2} + \frac{\hbar^2\omega'^2}{c^2} - \frac{2\hbar^2\omega\omega'}{c^2} \cos\theta = p_e'^2 \quad (41)$$

Combining Eqs. (39) and (41) yields

$$\omega' = \frac{\omega}{1 + (\hbar\omega/mc^2)(1 - \cos\theta)} \quad \text{or} \quad \lambda' = \lambda + \frac{2\pi\hbar}{mc}(1 - \cos\theta) \quad (42)$$

Note that the wavelength of the scattered photon depends on the scattering angle. Also, the wavelength shift is independent of the initial wavelength. The shift only becomes significant for fairly short initial wavelengths, and hard (high-energy) X-rays must be used to see the effect.

#### 12.5.2.3 Raman Scattering

For a photon to couple to one of the collective nonlocalized vibrational modes of a lattice, momentum must be conserved. A photon traversing a material can emit or absorb an optical phonon, but in order to conserve momentum and energy, the frequency and direction of the photon must change. If a phonon is created, the interaction is called a *Stokes process*. If a phonon is absorbed, it is

an anti-Stokes process (Figure 12.7). Conservation of energy requires  $\omega = \omega' \pm \Omega$  where  $\omega$  is the frequency of the incident photon,  $\omega'$  is the frequency of the scattered photon, and  $\omega$ : is the frequency of the phonon that is created or absorbed by the photon. To conserve momentum,  $\mathbf{k} = \mathbf{k}' \pm \mathbf{K}$ , where  $\mathbf{k}$ ,  $\mathbf{k}'$ , and  $\mathbf{K}$  are the wave vectors for the incident photon, scattered photon, and phonon, respectively.

#### 12.5.2.4 Two-Phonon Absorption

Similarly, a photon cannot be completely absorbed into a single phonon because a phonon with the same energy will not have the same wave vector. In order to conserve momentum, the photon must create two phonons (Figure 12.8).

#### 12.5.2.5 Resonant Bond Breaking

Desorption induced by electronic transitions (DIET) (see Section 12.3.2.4) is possible with photons as well (Tolk *et al.*, 1983). If the incident photon has the appropriate resonant energy to excite an electron initially in a bonding state to an antibonding state, the bond may be broken.

#### 12.5.2.6 Laser Ablation

An incident photon may liberate electrons and desorb ionized target atoms. With a high-intensity laser beam, electrons and ions may be created in sufficient quantity to make a dense plasma near the surface of the target. Once the plasma exists, the laser may couple directly to the plasma, and the superheated plasma then ablates the target by collisions with plasma particles.

#### 12.5.2.7 Exciton Creation

If photons are incident on a semiconducting material, and the photon energy is slightly below the energy of the material's band gap, an electron may be excited

from the material's valence band to an energy level immediately below the band gap, where it will form, with the resulting hole, a bound pair state very similar to a hydrogen atom. This bound state is called an *exciton* (Kittel, 2004).

#### 12.5.2.8 Pockels and Kerr Effects

Under intense photon irradiation, materials may experience a change in their refractive indices, although the effect is generally very weak. There are some materials, however, where the effect is very strong. If  $\lambda$  is the wavelength of light to be refracted,  $K$  is a measure of the strength of the Kerr effect in the material (the Kerr constant), and  $E$  is the electric field due to the photon irradiation, the change in refractive index is given as

$$\Delta n = \lambda K |E|^2 \quad (43)$$

#### 12.5.2.9 Coherent Phonon Generation

Massive excitation of electron energy levels through photon bombardment may result in coherent multiple phonon generation as the excited electrons rapidly decay to the conduction band, shedding phonons in the process. This coherent acoustic phonon (CAP) wave may be used to probe materials and activate interesting events (Xu *et al.*, 2008).

#### 12.5.2.10 Sum Frequency Generation

In certain nonlinear media under intense photon irradiation, photons with frequencies higher than the incident photon frequencies may be produced in the material itself. If the material is under irradiation of two or more frequencies, the resulting photon frequency may be any of the sums of the incoming frequencies. For instance, if the incoming frequencies are  $\omega_1$  and  $\omega_2$ , the resulting frequency could be

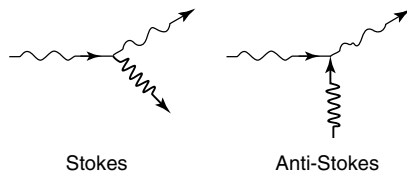


Fig. 12.7 Raman processes.

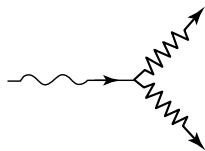


Fig. 12.8 Two-phonon absorption.

$\omega_1 + \omega_2$ . This is sum frequency generation. If the material is under monochromatic irradiation with frequency  $\omega$ , the resulting radiation may have a frequency of  $2\omega$  or even  $3\omega$ ; these special cases are called *second-* and *third-harmonic generation*, respectively (Shen, 2002).

### 12.5.3 Applications

#### 12.5.3.1 Scattered or Absorbed Incident Light

Photons with energies resonant with electronic transitions in the target will be strongly absorbed. Thus, if the transmission of light as a function of frequency is measured, the electronic structure of the target may be indirectly mapped. This is the basis of absorption spectroscopy. Because the resonances correspond to the difference in energy of two electronic states, rather than the absolute energy of a single electronic state, the information is somewhat convoluted. However, absorption spectra for most materials are well known, and so information about the target can be obtained without a detailed knowledge of the electronic structure. If the target is not transparent, the same information can be inferred from reflection.

#### 12.5.3.2 Electrons from the Target

In order to map the electronic states directly, the energy of photoelectrons can be measured. Since the energy of a photoelectron is just the energy of the photon minus the electron-binding energy, the spectrum of photoelectron energies is a direct measure of the electronic states of the target. This is the basis of X-ray photoelectron spectroscopy (XPS). However, this will only indicate filled states. In order to map the normally empty excited states, the excited states can be populated prior to measurement in a pump-probe experiment. For example, the density of states of the conduction band in a semiconductor can be mapped in this manner.

In semiconductors, some of the electronic structure of the target can be directly mapped without reverting to X-rays as in XPS. If a target is biased with a small voltage and the current flow is measured, the current will be enhanced when photons promote electrons to the conduction band. If this photocurrent is measured as a function of photon energy, the derivative of the resulting spectrum is a direct map of the density of states below the band gap. This is the basis of internal photoemission (IPE) spectroscopy. The simplicity

of the measurement and the lower photon energy make this method preferable to XPS.

The energy spectrum of photoelectrons will also have some additional structure. This is due to a characteristic energy loss as an electron is liberated from an inner shell, coupled with an interference effect as the photoelectron interacts with target atoms as it escapes from the target. This is the basis of extended X-ray absorption fine-structure (EXAFS) measurements. The advantage of EXAFS is the extremely localized sensitivity due to the short range of electrons in solids. Thus, the primary peak indicates the species of the scattering atom from the characteristic energy loss, and the fine structure indicates the lattice positions of its neighbors.

#### 12.5.3.3 Measuring Scattered Light

Since the phonon-dispersion relation is a unique function of the target material, Raman scattering will also be unique to the target material. The shift in energy of a scattered photon is a direct measure of the energy of the optical phonon with wave vector nearly equal to zero. This is the basis of Raman spectroscopy. If the incident beam is focused to a small spot, the identity of crystallites in a heterogeneous target may be spatially mapped as well.

Exactly as in the electron case, the diffraction pattern of X-rays scattered from a crystalline target is a measure of the long-range order of the target. This is the basis of X-ray diffraction.

#### 12.5.3.4 Mode Locking Lasers

The optical Kerr effect may be used to create self-focusing ultrafast lasers. If a material with a strong Kerr constant (a Kerr lens) is employed in a laser cavity, the

stronger standing wave modes in the laser cavity are more tightly focused, and the weaker modes may be therefore filtered out by geometric means, with the result that the strongest modes become stronger and the weaker modes disappear. This is the phenomenon of mode locking.

## 12.6 Neutron Impact

### 12.6.1

#### Interaction Mechanisms

##### 12.6.1.1 Scattering from Target Nuclei

Unlike ions or electrons, Coulomb scattering does not apply to neutrons because of their charge neutrality. A complete discussion of the neutron-scattering process is not possible here, but a few points should be made. A neutron can only scatter from the atomic nuclei in the target, which means neutron scattering is insensitive to the electronic structure of the target material. Since the cross section for neutron scattering is relatively small, neutrons usually penetrate well into the target, and neutron bombardment consequently is not surface sensitive. In addition, the scattering amplitude depends on the relative orientations of the neutron spin and nuclear spin so that a polarized neutron beam is sensitive to magnetization. In many cases, neutron beams may have very low energies of less than 0.1 eV per particle. With other beam particles, interactions could be treated as simple two-particle collisions. For a low-energy neutron beam, this is not the case. In fact, interactions with phonons dominate.

##### 12.6.1.2 Elastic Scattering from a Lattice

A low-energy neutron may also scatter from the nuclei in the target as a

whole. As in the case of electrons, this elastic scattering results from the wave nature of the neutron, and as before, quantum interference effects result. For constructive interference, the Bragg condition must be satisfied, and specific scattering angles are preferred, resulting in a diffraction pattern. Note that the Bragg condition depends on the de Broglie wavelength, which in turn depends upon the energy. Thus, while electrons are much preferred for diffraction studies, neutron diffraction is still very important as a means of monochromatizing a neutron beam.

### 12.6.1.3 Neutron Activation

For many target atoms, energetic neutron bombardment may produce a nuclear reaction, resulting in an unstable isotope (see Chapter 10). The unstable isotope will then decay producing radiation. Since the target is now said to be “radioactive” or “activated,” this process is called *neutron activation*. If  $N_x$  is the number of atoms available to be activated in the target and  $N_y$  is the number of activated atoms, then the growth of the number of activated nuclei is given by

$$\frac{dN_y}{dt} = N_x \sigma \phi - N_y \lambda_y \quad (44)$$

where  $\sigma$  is the reaction cross section,  $\phi$  is the flux of neutrons, and  $\lambda_y$  is the decay constant of the unstable nuclei. The first term in this equation is the rate of activation, while the second term is the rate of decay of already activated atoms. Integrating this gives the number of activated atoms as a function of the time of bombardment  $t$ :

$$N_y = \frac{N_x \sigma \phi}{\lambda_y} (1 - e^{-\lambda_y t}) \quad (45)$$

The activity  $A_t$ , which is the number of decays per second, is just the number of activated atoms times the decay constant:

$$A_t = N_x \sigma \phi (1 - e^{-\lambda_y t}) \quad (46)$$

It is apparent that after a long bombardment time, the activity saturates. In fact, the activity reaches 50% of saturation in one half-life and 75% in two half-lives. This gives experimental control over other undesired processes. Processes with much longer half-lives than the desired reaction can be avoided by stopping activation after two half-lives. Processes with much shorter half-lives than the desired reaction may be eliminated by waiting to measure the activity until a full half-life after bombardment ceases.

## 12.6.2

### Neutron-Bombardment Phenomena

#### 12.6.2.1 Phonon Emission and Absorption

Excluding nuclear processes, a low-energy neutron will interact with target nuclei primarily by inducing normal-mode vibrations or phonons. In a given direction in a given lattice, only particular phonon energies and momenta are allowed. Since momentum must be conserved, neutrons will scatter most readily in those directions for which the change in momentum of the neutron corresponds to an allowed phonon in the lattice. In addition, during absorption or emission of a phonon, the lattice as a whole may give or take specific quantities of momentum as indicated by the reciprocal lattice vectors  $\mathbf{G}$ . Thus, if  $\mathbf{q}$  is the wave vector of an allowed phonon and  $\mathbf{k}$  is the propagation vector of the neutron, then the change in the propagation vector of the neutron  $\Delta\mathbf{k}$  satisfies the following

condition:

$$\Delta \mathbf{k} = \pm \mathbf{q} + \mathbf{G} \quad (47)$$

The plus–minus sign indicates that the neutron may either absorb or emit a phonon. The above condition specifically applies to the bulk phonon structure since neutrons penetrate deeply into the target, and neutron bombardment is not sensitive to surface phonons.

#### 12.6.2.2 Decay-Product Energy Loss

If the decay product of an activated nucleus is a charged particle, then it will lose energy as it escapes from the target through scattering from electrons in the target material. This is exactly the same as the electronic energy loss discussed in Section 12.4. Assuming that the fractional energy loss is small and that the target material is fairly uniform, the energy loss is found to be proportional to the distance traveled through the material. Decay-product energy loss differs from the Rutherford backscattering case in one very important way: the charged particle only has to travel through the target material once. Typically, these decay products have energies of a few mega electron volts and can escape from depths up to a few microns beneath the surface.

### 12.6.3

#### Applications

##### 12.6.3.1 Elastic Scattering

Diffraction of neutrons by a crystal depends on the energy of the neutrons. In order to produce low-energy neutron beams with well-defined energies, a beam of thermal neutrons is scattered from a crystal and collimated. The diffraction angle determines the energy and can be varied by

rotating the crystal and apertures. Neutron monochromators operate according to these principles.

##### 12.6.3.2 Inelastic Scattering

Measuring the scattering angle and energy of neutrons scattered from a crystal maps the phonon structure of the lattice. The change in momentum of the neutron corresponds to the momentum of the phonon, and the change in energy of the neutron is the energy of the phonon. Such measurements are routinely carried out with a triple-axis neutron spectrometer.

##### 12.6.3.3 Reaction Products

If the cross section for activation and the lifetime of the unstable isotope are known, then the concentration of a particular species in a target can be calculated directly from the measured activity. This is the basis of neutron activation analysis. Some care is necessary to reduce the background of other activation processes.

If the reaction product is a charged particle, then a depth profile of the activated species can be obtained by measuring the energy of the escaping particles. This is the basis of neutron activation depth profiling.

##### 12.6.3.4 Spallation

In addition to fusion- and fission-based neutron sources, a process known as *spallation* may be utilized to produce high-energy pulsed neutron beams. Firing 1.0 GeV protons (as opposed to decay product neutrons, as in a chain reaction) into a high atomic mass target releases tens of neutrons per proton as the target is vaporized. This provides an efficient source of pulsed neutrons for research purposes. The Spallation Neutron Source (SNS) at the Oak Ridge National Laboratory recently came online and represents the

most powerful neutron source available (Mason *et al.*, 2000).

## 12.7

### Conclusion

Particle impact onto condensed matter results in a great variety of phenomena. In this chapter, the most important effects have been presented, but these are by no means all of the possible results of an impact event. More importantly, the reader should understand that any given impact experiment will produce many of the phenomena described above. Experiments are usually designed to emphasize one particular aspect of the impact event. However, while an electron energy-loss experiment may emphasize plasmon excitation, the experimenter must be aware that the electron beam may also be diffracting, undergoing collision cascades, ejecting core electrons, creating electron-hole pairs, or producing lattice defects. It is this great variety of effects that makes directed particle or photon beams powerful probes for measuring the properties of materials.

### Glossary

**AES (Auger-Electron Spectroscopy):** An experimental technique for measuring the atomic species in the region near the surface of a solid by measuring the energies of Auger electrons.

**Anti-Stokes Process:** A Raman scattering process in which a photon is scattered by absorbing a phonon.

**Auger Electron:** An electron excited and possibly even liberated by the energy

released when another electron falls into a vacant low-energy state.

**Auger Process:** When an electron falls into a lower energy vacancy, energy is liberated. If that energy is transferred to another electron, resulting in that electron being excited to a higher state or the vacuum state, the process is called an *Auger process*, and the excited electron is called an *Auger electron*.

**Bragg Reflection:** The reflection of light or particles from parallel planes that have spacing such that self-interference determines the allowed scattering angles.

**Bremsstrahlung:** German for “braking radiation.” Bremsstrahlung is the broad spectrum of electromagnetic radiation produced when charged particles are decelerated by impact with a target.

**Channeling:** Phenomenon in which particles incident on a crystal in a high-symmetry direction reach unusually great depths by traveling through the spaces between the atoms.

**Coster-Kronig Transitions:** A particular Auger transition in which the vacancy is filled by an electron from the same subshell.

**Coulomb Scattering:** A model for scattering of charged particles in which the Coulomb repulsion or attraction due to the electric charge is assumed to dominate.

**Depth Profiling:** A technique in Rutherford backscattering experiments that exploits the nearly uniform deceleration of a charged particle in a solid to map the distribution of atomic species as a function of depth into the target.

**DIET (Desorption Induced by Electronic Transitions):** The ejection of an atom or molecule from a surface by a repulsive Coulomb force resulting from an electronic excitation.

**Diffraction Pattern:** The interference pattern produced at a detector or phosphor screen by particles or light elastically scattered from a lattice.

**Dipole Approximation:** Approximation of the interaction of light with electronic states that only considers the dipole term in the expansion of the electronic state.

**EELS (Electron Energy-Loss Spectroscopy):** An experimental technique for determining the electronic structure of a material by measuring the change in energy of a beam of electrons as they pass through a material.

**EMA (Electron Microprobe Analysis):** An experimental technique in which a tightly focused electron beam produces vacancies in the target atoms, and the radiation produced when other electrons fill the vacancies is spectroscopically analyzed.

**EXAFS (Extended X-Ray Absorption Fine Structure):** An experimental technique for measuring the lattice structure in the neighborhood of a particular impurity by carefully measuring the energy of photoelectrons produced by X-rays.

**Exciton:** In a semiconducting material, an electron and hole that are bound in a hydrogen-like state.

**Fermi's "Golden Rule":** An approximation of the probability of a photon producing a particular electronic transition calculated by treating the photon as a short-lived oscillatory perturbation and considering only dipole interactions.

**FRS (Forward Recoil Spectroscopy):** An experimental technique for measuring light atomic species in a thin film by measuring the energy of particles ejected in the forward direction by a high-energy ion beam.

**HREELS (High-Resolution Electron Energy-Loss Spectroscopy):** An experimental technique for measuring the electronic structure of the surface of a solid by measuring the change in energy of a low-energy beam of electrons reflected from a surface.

**Impact Parameter:** The perpendicular distance from the target particle to the initial line of flight of the incident particle.

**Impulse Approximation:** An approximation based on the assumption that the interaction between a fast-moving beam particle and a stationary target particle happens so quickly that neither particle has time to change its initial motion much while the interaction is occurring.

**IPE (Internal Photoemission):** An experimental method for mapping the density of states of the valence band of a semiconductor by measuring the photocurrent produced by a tunable light source.

**Kinematic Factor:** In an elastic two-particle collision, the fraction of energy retained by the incident particle.

**LEED (Low-Energy Electron Diffraction):** An experimental technique for measuring the near-surface lattice structure of a crystal by diffracting a low-energy beam of electrons from the surface.

**LEIS (Low-Energy Ion Spectroscopy):** An experimental technique for measuring the atomic species near the surface of a solid by reflecting a low-energy beam of ions from the surface and measuring the ion energy electrostatically.

**Mean Free Path:** The average distance traveled between interactions.

**Mode locking:** A laser generation technique where weaker pulses are filtered out of the laser cavity allowing the stronger pulses to become even stronger.

**Neutron Activation Analysis:** An experimental technique for measuring the concentration of atomic species in a sample by neutron bombardment activation.

**Phonon:** A collective vibration of a lattice that carries momentum and energy and is therefore treated as a virtual particle.

**PIXE (Proton- or Particle-Induced X-Ray Emission):** An experimental technique for measuring the atomic species in a target, in which particle bombardment produces vacancies in the target atoms, and the radiation produced when other electrons fill the vacancies is spectroscopically analyzed.

**Plasmon:** A collective oscillation of the electrons of a material, which carries momentum and energy and is therefore treated as a virtual particle.

**Quantum Interference:** Interference effects that result from the quantum wave nature of particles.

**Raman Scattering:** Photon scattering from the lattice either producing or absorbing a phonon.

**Reconstruction:** The rearrangement of the lattice structure at the surface of a crystal into a symmetry that differs from the bulk solid.

**RBS (Rutherford Backscattering):** An experimental technique for determining the atomic species in a target by measuring the energy of reflected ions.

**RHEED (Reflection High-Energy Electron Diffraction):** A convenient technique for determining the surface structure of a sample by diffracting a grazing-incidence high-energy beam of electrons from the surface.

**Scattering Angle:** The angle between the initial line of flight continued through the scattering center and the subsequent line of flight.

**Second Harmonic Generation:** The process by which photons with a doubled frequency is produced from a material under irradiation by a single original frequency.

**Spallation:** The splitting of heavy atoms into smaller nucleons by a proton or ion beam. Provides an efficient source of pulsed neutrons.

**Spectral Intensity:** The radiative power per unit frequency.

**Sputtering:** The ejection of target atoms from a surface by collision cascade.

**Sputtering Yield:** The number of target atoms sputtered from the surface per incident particle.

**Stokes Process:** A Raman process in which a photon is scattered from the lattice by emitting a phonon.

**Stopping Power:** The distance rate of energy loss normalized to the number of atoms.

**TEM (Transmission Electron Microscopy):** The classic electron microscopy in which a high-energy beam of electrons is passed through a very thin sample and the beam is then imaged on a phosphor screen.

**XPS (X-Ray Photoemission Spectroscopy):** An experimental technique for determining the electronic density of states of a sample by measuring the energy of photoelectrons produced by X-rays.

## References

- Behrisch, R. (ed.) (1981) *Sputtering by Particle Bombardment I*, Springer-Verlag, New York.
- Bethe, H. and Heitler, W. (1934) On the stopping of fast particles and on the creation of positive electrons. *Proc. R. Soc. London Ser. A*, **146**(856), 83–112.
- Feldman, L. and Mayer, J. (1986) *Fundamentals of Surface and Thin Film Analysis*, North-Holland, New York.

- Fetter, A. and Walecka, J. (1980) *Theoretical Mechanics of Particles and Continua*, McGraw-Hill, New York.
- Humphreys, F.J. (2004) Reconstruction of grains and subgrains from electron backscatter diffraction maps. *J. Microsc.*, **213**(3), 247–56.
- Jackson, J.D. (1999) *Classical Electrodynamics*, 3rd edn, Wiley-VCH Verlag GmbH.
- Jespergard, P. and Davies, J.A. (1967) *Can. J. Phys.*, **45**, 2983–94.
- Kittel, C. (2004) *Introduction to Solid State Physics*, 8th edn, Wiley-VCH Verlag GmbH, New York.
- Mason, T.E. *et al.* (2000) The spallation neutron source: a powerful tool for materials research, *LINAC 2000* paper FR203.
- Ozbyay, E. (2006) Plasmonics: merging photonics and electronics at nanoscale dimensions. *Science*, **5758**, 189–93.
- Shankar, R. (1994) *Principles of Quantum Mechanics*, 2nd edn, Springer, New York.
- Shen, Y.R. (2002) *The Principles of Nonlinear Optics*, Wiley Interscience.
- Tolk, N. *et al.* (1983), *Desorption Induced by Electronic Transitions*, Springer-Verlag, New York.
- Wichmann, E. (1971) *Quantum Physics*, McGraw-Hill, New York.
- Xu, Y. *et al.* (2008) Pump-probe studies of travelling coherent longitudinal acoustic phonon oscillations in GaAs. *Physica Status Solidi (C)*, **5**(8), 2632–36.

## Further Reading

### General

- Prutton, M. (1994) *Introduction to Surface Physics*, Oxford Science Publications, Oxford.
- Woodruff, D.P. and Delchar, T.A. (1994) *Modern Techniques of Surface Science*, 2nd edn, Cambridge Univ. Press, New York.

## Electron Impact

- Bundle, C.R. and Baker, A.D. (eds) (1981) *Electron Spectroscopy: Theory, Techniques and Applications*, Academic Press, New York.
- Ibach, H. (ed.) (1977) *Topics in Current Physics*, Vol. 4, Springer-Verlag, Berlin.

## Ion Impact

- Tesner, J.R. and Natasi, M. (eds) (1995) *Handbook of Modern Ion Beam Analysis*, Materials Research Society, Pittsburgh.
- Tolk, N.H., Traum, M.M., Tully, J.C., and Madey, T.E. (eds) (1983) *Desorption Induced by Electronic Transitions, DIET I*, Springer-Verlag, New York.

## Photon Impact

- Cohen-Tannoudji, C., DupontRoc, J., and Grynberg, G. (1992) *Atom-Photon Interactions*, Wiley-VCH Verlag GmbH, New York.
- Kienzle-Focacci, M.N. and Wadhwa, M. (eds) (2001) *PHOTON 2001: Proceedings of the International Conference on the Structure and Interactions of the Photon Including the 14th International Workshop on Photon-Photon Collisions*, World Scientific Publishing Co. Ltd, Singapore.

## Neutron Impact

- Izyumov, Y.A. and Chernoplekov, N.A. (1992) *Neutron Spectroscopy*, Consultants Bureau, New York.
- Skold, K. and Price, D.L. (1986) *Neutron Scattering*, Part A, Vol. 23, Academic Press, Boston.

